Input-Reflectionless Out-of-Phase 3-dB Bandpass Filtering Couplers

Roberto Gómez-García[1], José-María Muñoz-Ferreras[1], and Dimitra Psychogiou[2]

[1]Dpt. Signal Theory and Commun., University of Alcalá, Alcalá de Henares, 28871, Madrid, Spain
[2]Dpt. Electrical, Computer, and Energy Eng., University of Colorado Boulder, Boulder, CO 80309, USA

***Abstract*— A class of out-of-phase 3-dB bandpass-filtering couplers with input-reflectionless capabilities is presented. To obtain the bandpass-filter (BPF) functionality, identical BPF sections are respectively co-integrated in the coupler signal paths from the input to the direct and coupled ports. Furthermore, a resistively-terminated bandstop-filter (BSF) section with complementary transfer function with regard to the one of the BPF section is loaded at the coupler input access. In this manner, the RF input-signal energy that is not transmitted to the direct and coupled terminals is dissipated by the loading resistor of the BSF section. Hence, the input-reflectionless behavior is realized. Optimization-based first-to-third-order design examples are shown. Moreover, for practical-validation purposes of this RF tri-functional device, a 2-GHz second-order microstrip prototype is built and tested.**

I. Introduction

Microwave 3-dB directional couplers or hybrid couplers are four-port reciprocal passive networks that distribute the input-signal energy between their direct and coupled ports whereas the remaining terminal is isolated [1]. They find use in various RF applications, such as the design of feeding networks for antenna beamforming or reflection-type phase shifters. Recently, 3-dB couplers are being co-integrated with other RF analog-signal-processing actions—e.g., filtering or amplification—in the same device. Benefits of this multi-functional design approach include reduced circuit size/volume, lower insertion loss, and optimized RF performance with the co-synthesis [2].

In the case of 3-dB bandpass filtering couplers with out-of-phase signals in their direct and coupled ports, some exponents to be highlighted are those in [3]–[8]. They include moderate- and high-order schemes for single- and multi-band designs with static and frequency-tunable response developed in different technologies—e.g., planar and 3-D substrate-integrated cavity resonators. All of them feature a reflective-type BPF behavior, so that the RF-input-signal energy that is not distributed to their direct and coupled ports within the bandstop regions is reflected back at the input. However, these unwanted RF-signal-power reflections may produce adverse effects into the preceding active stages, such as frequency-conversion modules—e.g., generation of additional unwanted intermodulation products through the remixing of such RF power reflections with the local oscillator—or power amplifiers—e.g., instability issues [9]. This may lead to the malfunctioning of the overall RF front-end chain. Note also that the use of inter-block isolation stages to alleviate this problem may be an inefficient alternative as they are bulky and hard to integrate.

In this work, a type of input-reflectionless out-of-phase 3-dB filtering bandpass couplers with input-reflectionless characteristics are reported by the first time. They exploit the reflectionless bandpass-filter (BPF) concept in [10] for this class of filtering couplers, by inserting a quasi-absorptive bandstop-filter (BSF) section at the input terminal that consumes in its loading resistor the RF-input-signal energy not transmitted by the coupler filtering electrical paths. The operational foundations and optimization-based theoretical design examples for this RF tri-functional circuit—i.e., 180º 3-dB coupling, bandpass filtering, and out-of-band isolation—are provided. Furthermore, for practical-validation purposes, a second-order microstrip prototype at 2 GHz is manufactured and measured.

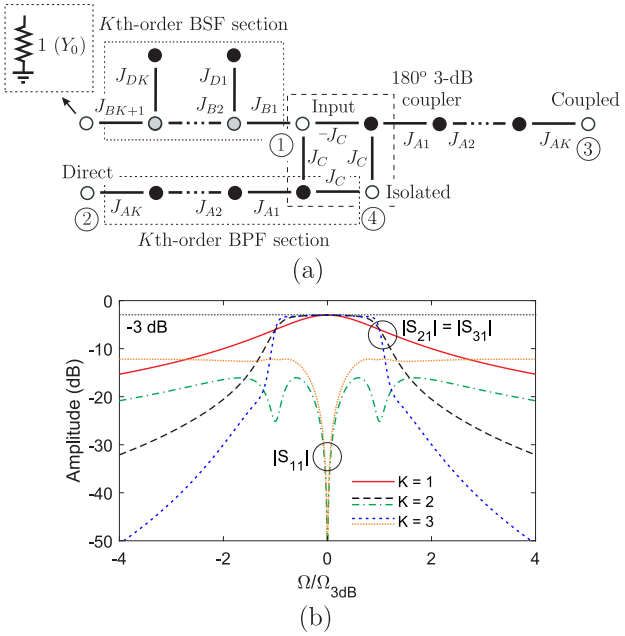

Fig. 1. (a) Normalized coupling-routing diagram of the proposed Kth-order input-reflectionless out-of-phase 3-dB bandpass-filtering coupler [black circles: resonating nodes; grey circles: zero-susceptance non-resonating nodes (NRNs) or connection points; white circles: unitary input, direct, coupled, and isolated ports and unitary loading resistor; continuous lines: admittance inverters; J variables: normalized admittance-inversion constants; and $Y_0 = 1/Z_0$: reference admittance for normalization]. (b) Examples of theoretical power transmission ($|S_{21}| = |S_{31}|$) responses from the input to the direct and coupled ports and input-reflection ($|S_{11}|$) responses for first-to-third-order examples (Ω: normalized frequency variable; Ω_{3dB}: 3-dB normalized cut-off frequency).

II. Theoretical Foundations

The circuit detail of the engineered input-reflectionless out-of-phase 3-dB bandpass-filtering coupler architecture is shown

978-1-5386-5944-1/19/$31.00 ©2019 IEEE

in Fig. 1(a). For a Kth-order implementation, it is composed of a 180^{o} 3-dB directional coupler in which Kth-order filtering sections are co-integrated as follows:

- Two identical Kth-order BPF sections are combined with the out-of-phase 3-dB coupler signal-propagation paths from its input to its direct and coupled ports, respectively, where the admittance inverters of the coupler are also exploited as source-to-first-resonator admittance inverters of the BPF sections. As a result, a Kth-order bandpass-filtering functionality is realized in the coupler. Furthermore, a perfect output power isolation between the direct and coupled ports is attained at all frequencies.
- A resistively-terminated Kth-order BSF section exhibiting a complementary filtering response with regard to the one of the BPF sections is connected to the coupler input port. In this manner, instead of being reflected back at the input, the RF-signal energy that is not distributed to the direct and coupled ports in the bandstop regions of the bandpass transmission responses is routed to the loading resistor of the input BSF section that dissipates it. Therefore, an input-reflectionless behavior is obtained.

For illustration purposes, several examples of theoretical power transmission and input-reflectionless parameters of the input-reflectionless out-of-phase 3-dB bandpass-filtering coupler topology in Fig. 1(a) for first-to-third-order cases are depicted in Fig. 1(b). They were derived by means of an inspection/optimization-based procedure in which: (i) the power transmission response was imposed to have the desired 3-dB transmission bandwidth and the degree of selectivity expected for such order, and (ii) the input-power-reflection parameter was minimized as much as possible. The resulting values for the admittance-inverter constants are summarized in Table I. As can be seen in Fig. 1(b), perfectly-zero input power reflection at any frequency is obtained for the first-order case whereas an input-quasi-reflectionless behavior is derived for the second- and third-order examples. In particular, as the order of the filtering functionality increases, both the filtering selectivity and the minimum input-power reflection level are augmented as a trade-off between selectivity/out-of-band rejection levels and input-reflectionless property. Note also that, at the normalized center frequency $\Omega = 0$, a perfect 3-dB power-division factor between the direct and coupled ports along with full power isolation between these terminals and total power matching at all ports is attained for all cases. The phase difference between the transfer functions from the input to the direct and coupled ports is 180^{o} at all frequencies.

TABLE I

DESIGN PARAMETER VALUES AND RESPONSE CHARACTERISTICS FOR THE THEORETICAL EXAMPLES IN FIG. 1(B)

K	Admittance Inverters	Ω_{3dB}	$\lvert S_{11}^{\max}\rvert$ (dB)	Behavior
1	$J_{A1}=1 \quad J_{B1}=1 \quad J_{B2}=1$ $J_C=1/\sqrt{2} \quad J_{D1}=1$	1	$-\infty$	Fully-reflectionless
2	$J_{A1}=1 \quad J_{A2}=1$ $J_{B1}=0.7275 \quad J_{B2}=0.7245$ $J_{B3}=1 \quad J_C=1/\sqrt{2}$ $J_{D1}=0.9525 \quad J_{D2}=1.3062$	1.308	-16.05	Quasi-reflectionless
3	$J_{A1}=1 \quad J_{A2}=1 \quad J_{A3}=1$ $J_{B1}=1.4246 \quad J_{B2}=2.1006$ $J_{B3}=1.8986 \quad J_{B4}=1$ $J_C=1/\sqrt{2} \quad J_{D1}=2.2484$ $J_{D2}=2.5171 \quad J_{D3}=1.8792$	1.592	-12.16	Quasi-reflectionless

III. EXPERIMENTAL RESULTS

To validate the practical viability of the proposed concept of input-reflectionless out-of-phase 3-dB bandpass-filtering coupler, the second-order example in Fig. 1(b) was manufactured in microstrip technology and characterized. For its design, a 2-GHz center frequency and a 3-dB absolute bandwidth of 385 MHz—i.e., equal to 19.3% in relative terms—were selected.

The transmission-line-based schematic of this circuit is represented in Fig. 2(a). The admittance inverters were realized as quarter-wavelength-at-2-GHz transmission-line segments whose characteristic impedances were finely adjusted from the theoretical ones—given by $Z = Z_0/J$—for performance optimization. Their final values are as follows ($Z_0 = 50\ \Omega$): $Z_{A1} = Z_0$, $Z_{A2} = Z_0$, $Z_{B1} = 7Z_0/5$, $Z_{B2} = 6Z_0/5$, $Z_{B3} = Z_0$, $Z_C = Z_0\sqrt{2}$, $Z_{D1} = Z_0$, and $Z_{D2} = 11Z_0/10$—note that the Z_{A2} and Z_{B3} inverters not shown in Fig. 2(a) were absorbed into the resistor and direct/coupled ports. The resonators were implemented as open-ended half-wavelength-at-2-GHz transmission-line segments with characteristic impedance $Z_r = 2Z_0/5$ to fulfill the bandwidth requisite. The theoretical S-parameters in amplitude are depicted in Fig. 2(b). As can be seen, owing to the frequency dependance of the admittance inverters, the input-reflectionless bandwidth is reduced to be more than twice the 3-dB transmission one. Fig. 2(c) demonstrates how the operational bandwidth can be flexibly adjusted through Z_r while maintaining the input-reflectionless behavior of the bandpass filtering coupler.

A photograph of the fabricated prototype is provided in Fig. 3(a). Its simulated—with Ansys HFSS—and measured—with an Agilent-E8361A network analyzer—S-parameters in amplitude are drawn in Fig. 3(b). The simulated and measured amplitude- and phase-imbalance curves between the direct and coupled ports are plotted in Fig. 3(c). As shown, a close agreement between simulations and measurements is obtained. The main measured characteristics of the built circuit are as follows: center frequency of 1.96 GHz, 3-dB absolute bandwidth equal to 345 MHz—i.e., 17.6% 3-dB relative bandwidth—, minimum in-band insertion-loss level of 3.63 dB and 3.93 dB for the direct and coupled ports—i.e., 0.63-dB and 0.93-dB excess loss with regard to the ideal 3-dB power-division factor—, minimum input-power-matching levels of 9.45 dB within the 1.59–2.28-GHz frequency range—i.e., twice the 3-dB transmission bandwidth—, and in-band power isolation above 23.1 dB. The measured in-band amplitude difference between the transmissions at the direct and coupled ports is in the range $(-0.31\ \text{dB}, +0.15\ \text{dB})$, whereas the in-band variation of their phase difference—with regard to the value at the center frequency—is in the interval $(-5.8^{\text{o}}, +5.3^{\text{o}})$.

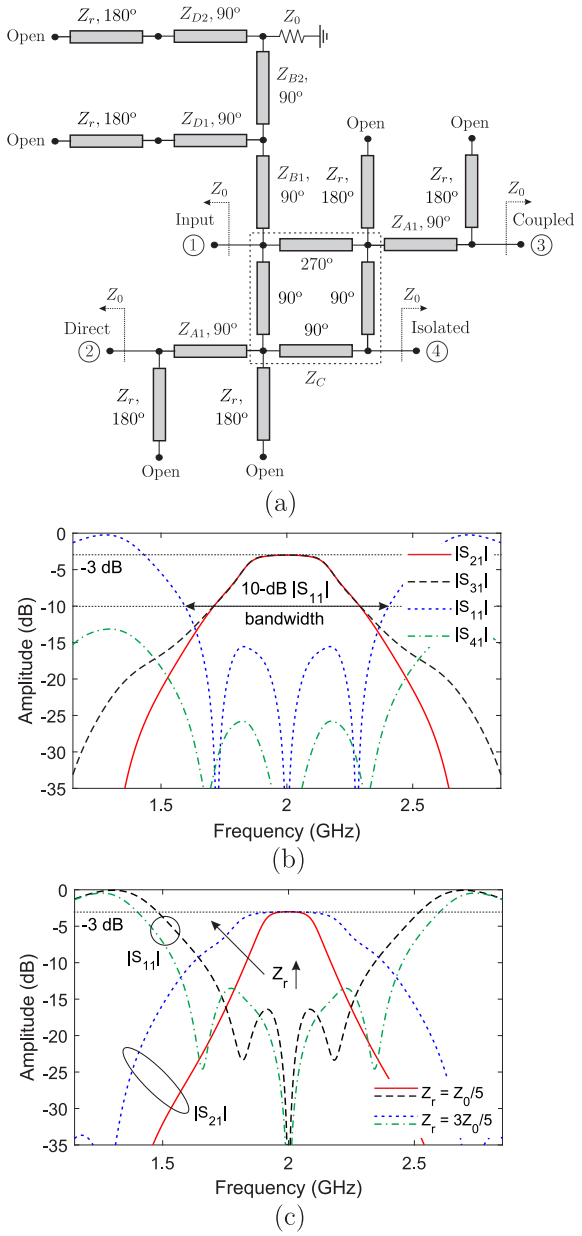

Fig. 2. Ideally-synthesized input-reflectionless out-of-phase 3-dB bandpass-filtering coupler. (a) Transmission-line-based circuit schematic. (b) Theoretical S-parameters in amplitude. (c) Bandwidth adjustment—in terms of $|S_{21}|$ and $|S_{11}|$—through the Z_r variable.

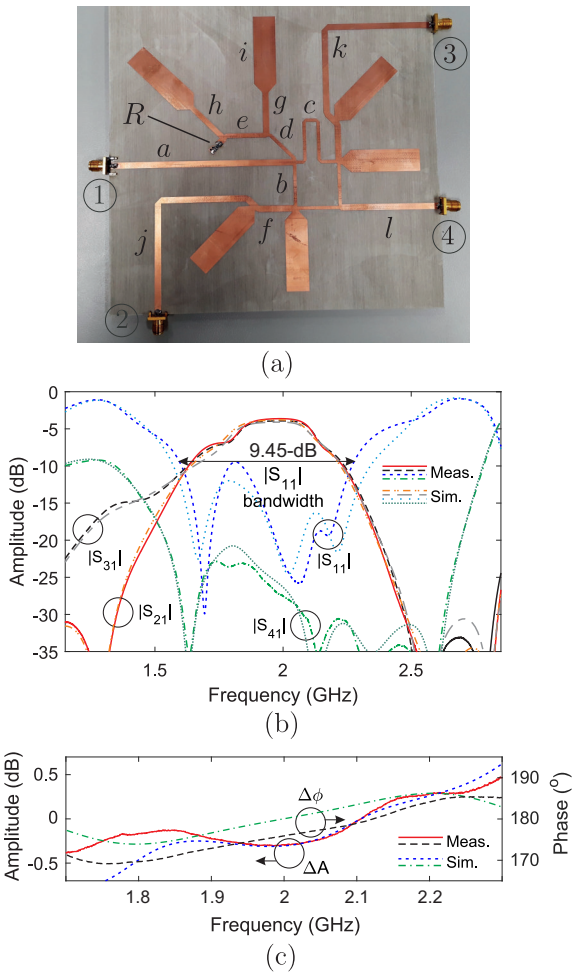

Fig. 3. Manufactured microstrip prototype of the input-reflectionless out-of-phase 3-dB bandpass-filtering coupler. (a) Photograph (Rogers RO4003C substrate: relative dielectric permittivity $\varepsilon_r = 3.38$, dielectric thickness $H = 1.524$ mm, metal thickness $t = 17.8$ μm, and dielectric loss tangent $\tan(\delta_D) = 0.0027$; dimensions in mm—"w" and "l" stand for width and length, respectively: $w_a = 3.5$, $l_a = 101$, $w_b = 1.9$, $l_b = 22$, $w_c = 1.9$, $l_c = 66.6$, $w_d = 1.9$, $l_d = 19.5$, $w_e = 2.6$, $l_e = 20.9$, $w_f = 3.5$, $l_f = 20.3$, $w_g = 3.5$, $l_g = 22.8$, $w_h = 3$, $l_h = 23$, $w_i = 12.5$, $l_i = 38$, $w_j = 3.5$, $l_j = 111.5$, $w_k = 3.5$, $l_k = 111.5$, $w_l = 3.5$, and $l_l = 53.8$; tapper length of resonating lines: 5 mm.). (b) Simulated and measured S-parameters in amplitude. (c) Simulated and measured amplitude-imbalance ($\Delta A = |S_{31}|/|S_{21}|$) and phase-imbalance ($\Delta\phi = |\sphericalangle\{S_{31}\} - \sphericalangle\{S_{21}\}|$) curves between direct and coupled ports.

IV. Conclusion

Out-of-phase 3-dB bandpass filtering couplers with input-reflectionless capabilities have been proposed by the first time. The theoretical operational foundations of this type of triple-functionality RF circuit have been described and illustrated with optimization-based theoretical design examples. Furthermore, a 2-GHz second-order microstrip prototype with a 10-dB input-reflectionless bandwidth that is twice its 3-dB transmission bandwidth has been developed and measured.

Acknowledgment

This work was financially supported in part by the Spanish Ministry of Economy, Industry and Competitiveness (State Research Agency) under Project TEC2017-82398-R and in part by the National Science Foundation under Award 1731956.

References

[1] G. Matthaei, L. Young, and E. M. T. Jones., *Microwave Filters, Impedance-Matching Networks, and Coupling Structures*. Norwood, MA: Artech House, 1980.

[2] N. Yang, C. Caloz, and K. Wu, "Greater than the sum of its parts," *IEEE Microw. Mag.*, vol. 11, no. 4, pp. 69–82, Apr. 2010.

[3] W.-R. Liu, T.-Y. Huang, C.-F. Chen, T.-M. Shen, and R.-B. Wu, "Design of a 180-degree hybrid with Chebyshev filtering response using coupled resonators," in *Proc. 2013 IEEE MTT-S Int. Microw. Symp.*, Seattle, WA, USA, Jun. 2–7, 2013, pp. 1–3.

[4] T.-W. Lin, J.-Y. Wu, J.- T. Kuo, "Filtering rat-race coupler with transmission zeros using compact miniaturized hairpin resonators," in *Proc.*

2015 IEEE MTT-S Int. Wireless Symp., Shenzhen, China, Mar. 30–Apr. 1, 2015, pp. 1–4.

[5] C.-H. Lin and J.-T. Kuo, "Compact eight-order microstrip filtering coupler," in *Proc. 2017 Asia-Pacific Microw. Conf.*, Kuala Lumpur, Malasya, Nov. 13–17, 2017, pp. 252–255.

[6] Y.-C. Lee, Y.-H. Pang, and H.-C. Huang, "A dual-band 180º hybrid coupler with a filter response," in *Proc. 2014 Asia-Pacific Microw. Conf.*, Sendai, Japan, Nov. 4–7, 2014, pp. 10–12.

[7] R. Gómez-García, J. Rosario-de Jesús, and D. Psychogiou, "Multi-band bandpass and bandstop RF filtering couplers with dynamically-controlled bands," *IEEE Access*, vol. 6, no. 1, pp. 32321–32327, 2018.

[8] M. F. Hagag and D. Peroulis, "A compact tunable filtering rat-race coupler," in *Proc. 2018 IEEE MTT-S Int. Microw. Symp.*, Philadelphia, PA, USA, Jun. 10–15, 2018, pp. 1–4.

[9] Mini-Circuits, Brooklyn, N.Y., "Reflectionless filters improve linearity and dynamic range," *Microw. J.*, vol. 58, no. 8, pp. 42–50, Aug. 2015.

[10] D. Psychogiou and R. Gómez-García, "Reflectionless adaptive RF filters: bandpass, bandstop, and cascade designs," *IEEE Trans. Microw. Theory Techn.*, vol. 65, no. 11, pp. 4593–4605, Nov. 2017.